Multi-Resonant Controller for Frequency-Varying Disturbance Rejection in Stewart Platforms ⋆

Jonathan Culau * **Rafael S. Castro** * **Guilherme A. Pimentel** **

* *Group of Automation and Control of Systems (GACS), Pontifical Catholic University of Rio Grande do Sul, Brazil*
** *Systems, Estimation, Control and Optimization Group (SECO), University of Mons, Belgium*

Abstract: This paper presents the design of a robust disturbance rejection control scheme for Stewart platforms. To fully take into account the system nonlinearities, the quaternion based description is used along with *Quasi*-Linear Parameter Varying representation. In order to provide robust output regulation, in the presence of frequency-varying disturbances, we propose the design of a multi-resonant internal model controller. The closed-loop stability is guaranteed by a state-feedback law synthesized via a convex optimization problem subject to linear matrix inequalities. Simulations show the effectiveness of the multi-resonant controller applied to a Stewart platform in the case that the platform is used as a stabilization device on the ocean, where the ocean waves generate frequency-varying harmonic disturbances.

Keywords: disturbance rejection; linear matrix inequalities; multi-resonant controller; quaternions; Stewart platform;

1. INTRODUCTION

The Stewart platform has several different applications, from motion platform for flight simulators (Villacis et al., 2017) to offshore cargo transfers (de Faria et al., 2016). The platform consists in a six degrees of freedom (6-DOF) parallel kinematic system given by a closed-kinematic chain (CKC) mechanism. Since it was proposed by Stewart (1966), the Stewart platform has been studied by many researchers. Due to the complexity of the Stewart platform dynamics, several methods such as Newton-Euler (Do and Yang, 1988), Lagrangian Formulation (Hajimirzaalian et al., 2010), Kane's equation (Liu et al., 2000), Quaternion-based Dynamic (de Faria et al., 2016) and Elman recurrent network (Guo et al., 2013) have been used for the analysis of this manipulator.

In the last three decades, disturbance rejection strategies have also been proposed, as inverse dynamic controller (IDC) (Lee et al., 2003), auto-disturbance rejection controller (ADRC) (Su et al., 2004). Normally, these methods use simplified models that inevitably have some modeling error, and the stability of the whole system cannot be guaranteed. In the other sense, adaptive control (Nguyen et al., 1993), sliding mode control (Kim and Lee, 1998), higher order sliding mode control (Kumar and Bandyopadhyay, 2012) schemes have been proposed to cope with the modeling errors, however these solutions still have the input chattering problem.

This chattering problem becomes an important issue when the application of the Stewart platform must deal with frequency-varying harmonic disturbances. Different control strategies can be found in the literature to handle this issue, for instance, Castro et al. (2017) proposed a solution to the frequency-varying version of the Resonant Controller for load reduction in wind turbines. In that paper, the state-feedback law is synthesized via an optimization problem subject to linear matrix inequalities (LMIs), which is a systematic way to design a controller, but there are very few studies using LMIs for Stewart platforms control (de Faria et al., 2016).

Considering these issues, this paper proposes a robust disturbance rejection scheme for Stewart platforms subjected to frequency-varying harmonics disturbances. In order to achieve the proposed goal, the dynamic equations of the platform must be represented in such a way that can be used in the LMI framework. For this reason we use an inverse kinematic quaternion-based model, which allow us to deal with the platform translational and rotational dynamics in a simple and straightforward way. In order to address the rotational nonlinearities of the platform, we propose to represent the system dynamics in a Quasi-linear parameter varying (Quasi-LPV) model, that allows us to use a linear design tool as the LMI framework in a complex nonlinear system (Rotondo et al., 2013) as the Stewart Platform.

The paper is organized as follows: Section 2 briefly presents quaternion representation as well as geometric and dynamic descriptions of the Stewart platform. Section 3 formally addresses the problem statement of the paper and Section 4 presents the proposed control design. Section 5 shows a numerical example and result discussion and Section 6 concludes the paper.

Notation: x_i is the i-th element of vector x. A_i is the i-th row of matrix A. $A^\top$ is the transpose of matrix A.

⋆ This work was supported in part by the Coordenação de Aperfeiçoamento de Pessoal de Nível Superior — Brasil (CAPES) — Finance Code 001.

$A > 0$ and $A < 0$ means respectively that matrix A is positive-definite and negative-definite. $\mathrm{diag}(A, B)$ denotes a diagonal matrix obtained by A and B. $\mathrm{tr}(A)$ is the trace of matrix A. $\mathrm{He}\{A\} := A + A^\top$ and $\star$ denotes symmetric elements in a matrix. $\mathcal{V}(\Delta)$ represents the vertices of the polytope Δ.

2. PRELIMINARIES

2.1 Quaternion Representation

A quaternion is originally defined as a extension of the complex domain and was proposed by W. R. Hamilton between 1844 - 1850. The vector form of quaternions can be represented as

$$q = \begin{bmatrix} \eta \\ \epsilon \end{bmatrix}, \tag{1}$$

where $\eta \in \mathbb{R}$ and $\epsilon \in \mathbb{R}^3$.

This representation simplifies analytical and numerical manipulations with angles, as presented in the following definitions.

Definition 2.1. (Quaternion Norm). The norm of q is defined as

$$||q|| = \sqrt{q^\top q}. \tag{2}$$

Definition 2.2. (Attitude Quaternion). A unit quaternion of the form

$$q = \begin{bmatrix} \cos(\phi) \\ r\sin(\phi) \end{bmatrix} \tag{3}$$

is an attitude quaternion and can be used to represent a rotation of angle ϕ around the unit vector $r \in \mathbb{R}^3$.

Definition 2.3. (Rotational Quaternion Matrix). Consider a vector $z \in \mathbb{R}^3$ in global coordinates, if $z' \in \mathbb{R}^3$ is the same vector in the rigid-body coordinates, then the follow relation holds:

$$z' = R(q)z, \tag{4}$$

where $R(q) \in \mathbb{R}^{3\times3}$ is the rotation matrix, given by:

$$R(q) = I + 2\eta S(\epsilon) + 2S^2(\epsilon), \tag{5}$$

where I is the 3×3 identity matrix and $S(x)$ is the skew-symmetric matrix function $S : \mathbb{R}^3 \to \mathbb{R}^{3\times3}$.

2.2 Stewart Platform

The Stewart platform consists in a 6-DOF parallel kinematic system given by a CKC mechanism. It has an static base platform and movable top platform, the latter also called end effector.

This system has three reference frames: a *global inertial frame* O_I and two *local reference frames*: one in the bottom platform O_B, and another in the top platform O_T. Both *local reference frames* have the coordinate origins coinciding with the center of mass of its respective body. Assuming that the global inertial frame origin coincides with the bottom platform local reference frame origin, and assuming that the perturbation applied on the bottom platform naturally propagates to the top platform, the there exists a Jacobian matrix which transforms the linear velocities of the six actuators $\dot{l} \in \mathbb{R}^6$ to the linear and angular velocities of the platform, as follows (de Faria et al., 2016):

$$\dot{l} = J \begin{bmatrix} \dot{p} \\ \omega \end{bmatrix}, \tag{6}$$

where $\dot{p} \in \mathbb{R}^3$ is the top platform linear velocity vector regarding the global inertial frame O_I and $\omega \in \mathbb{R}^3$ is the top platform angular velocity vector regarding the local reference frame O_T. The Jacobian matrix transpose $J^\top$ may also be used to relate the linear forces of the six actuators $f_l = [f_{l1} \dots f_{l6}]^\top$ to the forces and torques applied on the center of mass of the top platform (F_t and τ_t) that is

$$F = \begin{bmatrix} F_t \\ \tau_t \end{bmatrix} = J^\top f_l. \tag{7}$$

As a result of this Jacobian matrix (6), we can formulate the platform mathematical model disregarding the geometric aspect of the platform. Thus the platform dynamics can be represented as generic quaternion based 3D rigid body model, where the coordinate frame origin coincides with the center of mass (de Faria et al., 2016):

$$\begin{bmatrix} \dot{\epsilon} \\ \dot{\omega} \\ \dot{p} \\ \dot{\upsilon} \end{bmatrix} = \begin{bmatrix} \frac{1}{2}\left(\eta I + S(\epsilon)\right)\omega \\ -I_m^{-1} S(\omega) I_m \omega \\ \upsilon \\ 0 \end{bmatrix} + \begin{bmatrix} 0 & 0 \\ I_m^{-1} & 0 \\ 0 & 0 \\ 0 & m^{-1} \end{bmatrix} \left(\begin{bmatrix} u_\tau \\ u_F \end{bmatrix} + \begin{bmatrix} d_\tau \\ d_F \end{bmatrix} \right) \tag{8}$$

where $I_m \in \mathbb{R}^3$ is the inertia matrix, m is the top platform body mass, $u_\tau \in \mathbb{R}^3$ and $d_\tau \in \mathbb{R}^3$ are the input and exogenous perturbation torques referenced on the local body reference frame, $u_F \in \mathbb{R}^3$ and $d_F \in \mathbb{R}^3$ are the input and the exogenous perturbation force vector referenced on the global referenced frame that includes the gravity force. $\begin{bmatrix} \eta & \epsilon^\top \end{bmatrix}^\top$ is an attitude quaternion that represents the rigid body orientation, as the states variables η and ϵ are intrinsically connected by the unit quaternion constraint $\eta^2 + \epsilon^\top \epsilon = 1$, we may drop the variable η without any loss of generality, $\omega \in \mathbb{R}^3$ is the angular velocity vector, $p \in \mathbb{R}^3$ is the position vector, $\upsilon \in \mathbb{R}^3$ is the linear velocity vector. The exogenous signals d_τ and d_F are unmeasured, but their fundamental frequencies is assumed to be measured.

3. PROBLEM STATEMENT

Having all the above descriptions in mind, now we can formally address the problem statement. Considering the open-loop system representation, the perturbation signals d are generated by the exogenous system

$$\begin{cases} \dot{w} = \Psi(\delta) w \\ d = \Omega w \end{cases}, \tag{9}$$

where $w \in \mathbb{R}^{12h}$, $\Psi(\delta) \in \mathbb{R}^{12h\times12h}$, $\Omega \in \mathbb{R}^{6\times12h}$ and $\delta \in \Delta$ is the time-varying parameter vector, which is assumed to be measured and bounded by the following polytope $\forall\, t > 0$:

$$\Delta = \{\delta \in \mathbb{R} : \delta \in [\underline{\delta}, \overline{\delta}]\}. \tag{10}$$

It is essential that we describe the exogenous system (9) associated to the production of perturbation signals. In this study, we deal with periodic resonant disturbances, such as ocean waves, whose the dynamics can be simply described as follow:

$$\Psi(\delta) = \mathrm{diag}\left(\Psi_r(\delta), 2\Psi_r(\delta), \dots, h\Psi_r(\delta)\right). \tag{11}$$

$$\Omega = \text{diag}([1\ 0], \ldots, [1\ 0]) \tag{12}$$

where

$$\Psi_r(\delta) = \text{diag}\underbrace{\left(\begin{bmatrix} 0 & \delta \\ -\delta & 0 \end{bmatrix}, \ldots, \begin{bmatrix} 0 & \delta \\ -\delta & 0 \end{bmatrix}\right)}_{6 \text{ times}}, \tag{13}$$

where $\delta \in \Delta$ is the time-varying resonant frequency, h is the number of considered harmonics components.

Therefore, this work proposes a solution to the follow problem:

Problem 3.1. Design a control law such that the trajectories $x(t)$ of the closed-loop dynamics asymptotically approach the origin for some admissible set of initial conditions $(x(0), w(0)) \in D_x \times D_w \subseteq R^6 \times R^{12h}$ and admissible time-varying parameters $\delta \in \Delta$. Furthermore, we intend to guarantee the exponential convergence of $x(t)$ to zero within a minimum user-defined decay rate $\alpha > 0$.

4. PROPOSED CONTROL STRATEGY

4.1 Quasi-LPV Formulation

With the purpose to design the control via optimization problem subject to LMIs, the system dynamic equations must be represented in such a way that can be solved by convex tools. One of the ways to comply with this issue is to represent the system in the Quasi-LPV form. The Quasi-LPV representation can be defined as a linear time-varying plant, whose state-space matrices are functions of the system states vector itself. Now consider the following open-loop system representation

$$\begin{cases} \dot{x} = A(\theta(x))x + Bu + Bd \\ y = Cx \end{cases}, \tag{14}$$

where $A(\theta(x)) \in \mathbb{R}^{12\times12}$, $B \in \mathbb{R}^{12\times6}$ and $C \in \mathbb{R}^{6\times12}$ are the states space matrices, $x = \begin{bmatrix}\epsilon^\top & \omega^\top & p^\top & v^\top\end{bmatrix}^\top \in \mathcal{X} \subset \mathbb{R}^{12}$ is the system states vector, $u = \begin{bmatrix}u_\tau^\top & u_F^\top\end{bmatrix}^\top \in \mathbb{R}^6$ are the control inputs vector, $y \in \mathbb{R}^6$ is the system output vector, $\theta(x) = \begin{bmatrix}\eta & \omega^\top\end{bmatrix}^\top : \mathcal{X} \to \Theta$ is a vector of polytopic-bounded state-dependent parameters and $d = \begin{bmatrix}d_\tau^\top & d_F^\top\end{bmatrix}^\top \in \mathbb{R}^6$ is the unmeasured disturbance vector. Thereby, we can write the state-space matrices of the system (8) as follow

$$A(\theta(x)) = \begin{bmatrix} -\frac{1}{2}S(\omega) & \frac{1}{2}\eta I & 0 & 0 \\ 0 & I_m^{-1}S(\omega)I_m & 0 & 0 \\ 0 & 0 & 1 & 0 \\ 0 & 0 & 0 & 0 \end{bmatrix}, \; B = \begin{bmatrix} 0 & 0 \\ I_m^{-1} & 0 \\ 0 & 0 \\ 0 & m^{-1} \end{bmatrix},$$
$$C = \begin{bmatrix} I & 0 & 0 & 0 \\ 0 & 0 & I & 0 \end{bmatrix}. \tag{15}$$

The state-feedback control law of the Quasi-LPV system can be design by using the LMI framework, provided that we ensure the trajectories of the system states are contained inside the set $\forall\, t \geq 0$:

$$\mathcal{X} = \{x \in \mathbb{R}^{12} : |x_i| \leq \sin\left(\frac{\bar{\phi}}{2}\right) \; \forall\, i = 1,2,3, \; |x_i| \leq \bar{\omega} \; \forall\, i = 4,5,6\} \tag{16}$$

where $\bar{\phi}$ is the maximum admissible orientation angle and $\bar{\omega}$ denotes the maximum admissible angular velocity in every coordinate. Consequently, for each of the scheduling parameters in the vector θ, their minimum and maximum values over the allowed values of x are calculated:

$$\Theta = \{\theta \in \mathbb{R}^4 : \cos\left(\bar{\phi}/2\right) \leq \theta_1 \leq 1,\; |\theta_i| \leq \bar{\omega}, i = 2,3,4\} \;\forall\, t \geq 0. \tag{17}$$

Note that the polytope Θ is valid only if $0 \leq \bar{\phi} < \pi$, thus we will limit our analysis accordingly. The control law must ensure that the trajectories of $x(t)$ are contained in the set $\mathcal{X}$, consequently we will guarantee that the trajectories of θ are contained inside the set Θ.

4.2 Control Scheme

A perturbation signal can be asymptotically tracked or rejected if its dynamics are reproduced by the states of the controller, provided that the stability of the closed-loop system is ensured. The proposed closed-loop is illustrated by Figure 1, where the 'IM' block is the controller internal model given by:

$$\begin{cases} \dot{\xi} = \Phi(\delta)\xi + \Gamma y \\ u = H\xi + Kx \end{cases}, \tag{18}$$

where $\xi \in \mathbb{R}^{12h}$ is the control internal states vector. The gain matrices $K \in \mathbb{R}^{6\times12}$ and $H \in \mathbb{R}^{6\times12h}$ are obtained via a optimization problem subject to LMIs, the 'System Plant' block represents the dynamics given by (8) and the Jacobian matrix is represented by the J block, the 'Exogenous System' represent the dynamics from (11). With the internal model control, the open-loop dynamics of the system can be describe by the follow augmented system:

$$\dot{\mathbf{x}} = \begin{bmatrix}\dot{x} \\ \dot{\xi}\end{bmatrix} = \begin{bmatrix} A(\theta(x)) & 0 \\ \Gamma C & \Phi(\delta) \end{bmatrix}\mathbf{x} + \begin{bmatrix} B \\ 0 \end{bmatrix} u + \begin{bmatrix} B\Omega \\ 0 \end{bmatrix} w. \tag{19}$$

Considering the control law $u = Kx + H\xi$, thus the closed-loop dynamics can be defined as follow:

$$\dot{\mathbf{x}} = \begin{bmatrix} A(\theta(x)) + BK & BH \\ \Gamma C & \Phi(\delta) \end{bmatrix}\mathbf{x} + \begin{bmatrix} B\Omega \\ 0 \end{bmatrix} w. \tag{20}$$

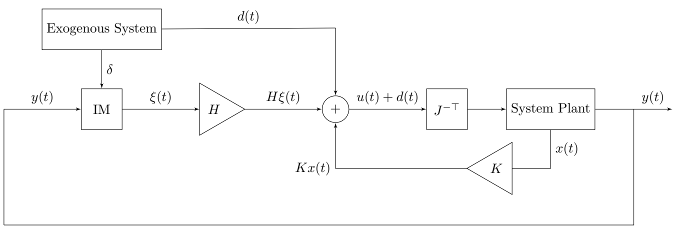

Figure 1. Proposed Control Loop Plant

4.3 Design of the Internal Model terms Φ and Γ

To solve the Problem 3.1 we must find conditions that guarantees a set $\mathcal{M}$ invariant and attractive, such that the output $y(t)$ will be zero inside $\mathcal{M}$. The following definition express these conditions.

Definition 4.1. (Center Manifold). A Center Manifold is defined as follows

$$\mathcal{M} = \{(x, \xi, w, \delta) \in \mathbb{R}^{12} \times \mathbb{R}^{12h} \times \mathbb{R}^{12h} \times \Delta : x = 0, \xi = \Sigma w\}, \tag{21}$$

which is said to be invariant with respect to the trajectory $(x(t), \xi(t), w(t))$ if

$$(x(t_0), \xi(t_0), w(t_0)) \in \mathcal{M} \Rightarrow (x(t), \xi(t), w(t)) \in \mathcal{M} \;\forall\, t > t_0, \tag{22}$$

and regionally attractive in $\mathcal{D}$ if

$$\lim_{t\to\infty}(x(t), \xi(t), w(t)) \in \mathcal{M}\ \forall\ (x(0), \xi(0), w(0)) \in \mathcal{D}\times\mathbb{R}^{12h}. \tag{23}$$

Consider the follow theorem that solves Φ and Γ ensuring the $\mathcal{M}$ invariance, such that the output y will be zero inside $\mathcal{M}$.

Theorem 4.2. Consider the augmented system (19), the $\mathcal{M}$ will be invariant if the output y is zero within it with the follow internal model:

$$\begin{cases}\Phi(\delta) = \Psi(\delta)\\ \Gamma = \text{diag}\left(\begin{bmatrix}1\\1\end{bmatrix}, \dots, \begin{bmatrix}1\\1\end{bmatrix}\right)\end{cases} \tag{24}$$

Proof. Consider the augmented system (19), the manifold $\mathcal{M}$ will be invariant with respect to the trajectories of the system (14) with the control internal structure (18), if the substitution of x by Πw and ξ by Σw is feasible. Thus Σ and Π must satisfy the follow regulator equations:

$$\begin{cases}\Pi\Psi(\delta) = A(\theta(x))\Pi + BU + B\Omega\\ \Sigma\Psi(\delta) = \Phi\Sigma(\delta) + \Gamma C\Pi \qquad \forall\,\delta\in\Delta,\ \forall\,\theta\in\Theta,\\ U = H\Sigma + K\Pi\end{cases} \tag{25}$$

where U is auxiliary variable, Π is the steady states map. Note that Π and Σ can be obtained by solving the follow Sylvester equation

$$\begin{bmatrix}\Pi\\ \Sigma\end{bmatrix}\Psi(\delta) = \begin{bmatrix}A(\theta(x)) + BK & BH\\ \Gamma C & \Phi(\delta)\end{bmatrix}\begin{bmatrix}\Pi\\ \Sigma\end{bmatrix} + \begin{bmatrix}B\Omega\\ 0\end{bmatrix}. \tag{26}$$

Therefore the unforced system stabilization ensures a uniqueness $\mathcal{M}$ descrbied by Σ and Π. Note that the regulators equation must satisfies the follow relation:

$$\Sigma\Psi(\delta) = \Phi\Sigma(\delta) + \Gamma C\Pi, \tag{27}$$

if we force $\Phi(\delta) = \Psi(\delta)$, the unique solution of the regulator equations is with $\Pi = 0$, in other words, the output y will be zero within $\mathcal{M}$.

The value of Γ must ensure that all internal model outputs are controllable by their inputs, thus we choosed a matrix filled by ones. ☐

4.4 LMI-based design of the feedback terms K and H

Now consider the follow coordinate changes

$$\mathbf{z} \triangleq \begin{bmatrix}x\\ \xi - \Sigma w\end{bmatrix}, \tag{28}$$

if we assume that $\mathcal{M}$ is invariant,the system dynamics can be described as follow

$$\dot{\mathbf{z}} = \begin{bmatrix}A(\theta(x)) + BK & BH\\ \Gamma C & \Phi(\delta)\end{bmatrix}\mathbf{z} = (\mathbf{A}(\theta(x), \delta) + \mathbf{BK})\mathbf{z}. \tag{29}$$

Noting that $\mathbf{K} = [K\ H]$ and the augmented state-space matrices are given by

$$\mathbf{A}(\theta(x), \delta) = \begin{bmatrix}A(\theta(x)) & 0\\ \Gamma C & \Phi(\delta)\end{bmatrix},\ \mathbf{B} = \begin{bmatrix}B\\ 0\end{bmatrix}. \tag{30}$$

Therefore, in order to $\mathcal{M}$ be regionally attractive in $\mathcal{D}$, we must ensure asymptotic stability of the system (29) for all $\mathbf{z}(0)$ inside the ellipsoid $\mathcal{D}$. Now let one consider the following theorem.

Theorem 4.3. Consider the closed-loop dynamics described by (29), a predefined scalars $\alpha > 0$ and κ. Suppose there exists a symmetric positive-definite matrix $\mathbf{F} \in \mathbb{R}^{n\times n}$ and a generic matrix $\mathbf{G}$ such that the following LMIs are satisfied:

$$\text{He}\{(\mathbf{A}(\theta, \delta)\mathbf{F} + \mathbf{BG}) + \alpha F\} < 0\ \forall\,\delta\in\mathcal{V}(\Delta), \theta\in\mathcal{V}(\Theta) \tag{31}$$

$$\begin{bmatrix}\sigma_i^2 & \mathbf{F}_i\\ \star & \mathbf{F}\end{bmatrix} > 0\ \forall\, i\in\{1, ..., 6\}, \tag{32}$$

$$\begin{bmatrix}-\kappa\mathbf{F} & \mathbf{A}(\theta, \delta)\mathbf{F} + \mathbf{BG}\\ \star & -\kappa\mathbf{F}\end{bmatrix} < 0\ \forall\,\delta\in\mathcal{V}(\Delta), \theta\in\mathcal{V}(\Theta), \tag{33}$$

where $\sigma = \begin{bmatrix}\sin(\bar\phi/2) & \sin(\bar\phi/2) & \sin(\bar\phi/2) & \bar\omega & \bar\omega & \bar\omega\end{bmatrix}^\top$. Then considering the feedback gain matrix

$$\mathbf{K} = \mathbf{G}\mathbf{F}^{-1} \tag{34}$$

it follows that the trajectories $x(t)$ of the closed-loop system exponentially approach the origin for every initial condition $\mathbf{z}(0)$ inside:

$$\mathcal{D} = \{\mathbf{z}\in\mathbb{R}^n : \mathbf{z}^\top\mathbf{P}\mathbf{z} \le 1\},\ \mathbf{P} = \mathbf{F}^{-1}. \tag{35}$$

where $n = 12 + 12h$.

Proof. Consider the follow Lyapunov candidate function

$$V(\mathbf{z}) = \mathbf{z}^\top\mathbf{P}\mathbf{z}, \tag{36}$$

for a symmetric and positive-definite matrix $\mathbf{P} \in \mathbb{R}^{n\times n}$. The exponential convergence of $x(t)$ to zero within a minimum user-defined decay rate $\alpha > 0$ can be satisfied if:

$$\alpha V(\mathbf{z}) + \dot V(\mathbf{z}, \delta) < 0 \forall\,\mathbf{z} \ne 0. \tag{37}$$

By evaluating $\dot V(\mathbf{z}, \delta)$ along the trajectories of system (19), we can rewrite (37) as:

$$\text{He}\{\mathbf{P}(\mathbf{A}(\theta, \delta) + \mathbf{BK}) + \alpha\mathbf{P}\} < 0, \tag{38}$$

which guarantees the target criteria. Now assume $\mathbf{z} \in \mathcal{X}\ \forall\, t \ge 0$, where:

$$\mathcal{X} = \{\mathbf{z}\in\mathbb{R}^n : |\mathbf{z}_i| < \sigma_i\}\ \forall\, i\in\{1, \dots, 6\}, \tag{39}$$

and σ is a vector with the maximum admissible values for the states vector $\mathbf{z}$. To ensure that this last condition is always true, we consider that the system initial state $\mathbf{z}(0)$ is within a positively-invariant set $\mathcal{D}\subset\mathcal{X}$, where

$$\mathcal{D} = \{\mathbf{z}\in\mathbb{R}^n : V(\mathbf{z}) \le 1\}, \tag{40}$$

consider the relation $\mathbf{z}_i = p_i\mathbf{z}$, so this last condition is ensured if

$$\left(\frac{\mathbf{z}_i}{\sigma_i}\right)^2 < \mathbf{z}^\top\mathbf{P}\mathbf{z} \le 1 \Leftrightarrow \mathbf{z}^\top\left(\frac{p_i^\top p_i}{\sigma_i^2}\right)\mathbf{z} < \mathbf{z}^\top\mathbf{P}\mathbf{z} \le 1. \tag{41}$$

From Schür's complement, the above relation becomes

$$\begin{bmatrix}\sigma_i^2 & p_i\\ \star & \mathbf{P}\end{bmatrix} > 0\ \forall\, i\in\{1, ..., 6\}. \tag{42}$$

Therefore, the trajectories $x(t)$ of the closed-loop system (19) exponentially approach the origin $\forall\,\mathbf{z}(0)\in\mathcal{D}$ if the matrix inequalities (38), (42) are satisfied. Additionally the aforementioned criteria, we limited the closed-loop (19) eigenvalues λ to a radius κ. Then consider the follow set

$$\mathcal{D}_r = \{\lambda_i\in\mathbb{C} : |\lambda_i| < \kappa\}\ \forall\, i\ \in\ \{1, \dots, n\}, \tag{43}$$

and put $\mathcal{D}_r$ in the form $\{\lambda\in\mathbb{C} : L + s\Upsilon + s^\star\Upsilon^\top < 0\}$ we have

$$|\lambda| < \kappa \Leftrightarrow \lambda\lambda^\star < \kappa^2 \Leftrightarrow < 0 \Leftrightarrow \begin{bmatrix}-\kappa & \lambda\\ \lambda^\star & -\kappa\end{bmatrix}. \tag{44}$$

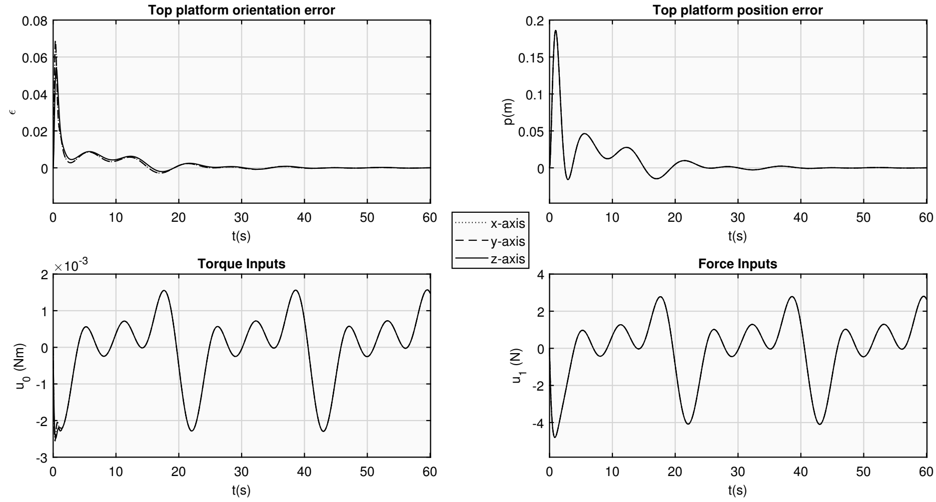

Figure 2. Simulation with $\delta = 0.3 rad/s$

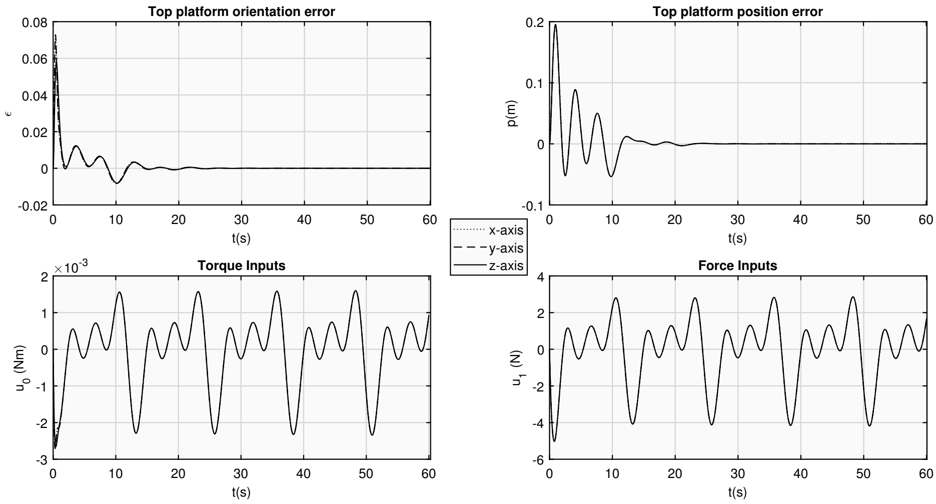

Figure 3. Simulation with $\delta = 0.5\ rad/s$

Therefore, the matrix L and Υ can be described as follow

$$L = \begin{bmatrix} -\kappa & 0 \\ 0 & -\kappa \end{bmatrix}, \quad (45)$$

$$\Upsilon = \begin{bmatrix} 0 & 1 \\ 0 & 0 \end{bmatrix}. \quad (46)$$

Considering the $\mathcal{D}$-Stability definition, we can formulate the follow constraint

$$\begin{bmatrix} -\kappa \mathbf{P} & \mathbf{P}\left(\mathbf{A}(\theta,\delta) + \mathbf{BK}\right) \\ \star & -\kappa \mathbf{P} \end{bmatrix} < 0 \; \forall \, \delta \in \Delta, \; \theta \in \Theta. \quad (47)$$

From convexity arguments, the relations (38), (42) and (47) also holds if we satisfies just on the vertices of the polytopes Θ and Δ. Also these relations are not LMIs with respect to decision variables $\mathbf{P}$ and $\mathbf{K}$. In order to circumvent this issue, let us introduce the following change of variables:

$$\mathbf{F} = \mathbf{P}^{-1}, \; \mathbf{G} = \mathbf{K}\mathbf{P}^{-1} \quad (48)$$

which yields the LMIs (31), (32) and (33). □

Based on Theorem 4.3, we propose to design K and H, such that the region of admissible initial conditions $\mathcal{D}$ is maximized. This can be achieved by solving the following convex optimization problem

$$\underset{\mathbf{F},\mathbf{G}}{\text{minimize}} \; \text{tr}(\mathbf{P}) \text{ subject to } \{\mathbf{F} > 0, (31), (32), (33)\}. \quad (49)$$

5. SIMULATION RESULTS AND DISCUSSION

This section presents two simulation results where we considered a top platform with $m = 1.36\ kg$ and $I_m = 10^{-4} diag\,(1.705,\ 1.705,\ 3.404)\ kgm^2$ (the simulation code is available at https://github.com/jonculau/sba-matlab). The initial conditions of the system and the exogenous generator were selected in such a way that $V(\mathbf{z}) \approx 0.9987$. The simulation with the initial values close to the border of the ellipsoid $\mathcal{D}$ proves that the trajectories does not leave the ellipsoid as expected for all initial values contained inside the set $\mathcal{D}$.

The controller was synthesized with $\alpha = 0.05$, $\kappa = 15$, $h = 3$, $\overline{\delta} = 0.5\ rad/s$ and $\underline{\delta} = 0.3\ rad/s$. Additionally, the bounds of Θ and $\mathcal{X}$ were calculated with a $\overline{\phi} = 25°$ and $\overline{\omega} = 5\ rad/s$.

Figures 2 and 3 illustrate two simulations varying the fundamental exogenous resonant frequency δ. In both simulations, the system had an expected behavior with a settling time smaller than 30 seconds for all system outputs. These simulations with the value of δ at the vertices of Δ prove that the multi-resonance internal model can reject any resonant disturbance up to the third harmonic with fundamental frequency within the polytope. The simulations also show that we guarantee the exponential convergence of the output $y(t)$ to zero within a minimum user-defined decay rate α without any input chattering problem. Note that, we considered a control internal model with the number of harmonics $h = 3$, a larger number would reduce the set of admissible initial conditions or would create a infeasible solution. Nonetheless, the simulation results show that the proposed control internal structure rejects all disturbances generated by a exogenous system with the same eigenvalues of the term Φ.

Also, it is important to mention that in this work we design the controller for the complete system (translation + orientation), but the Jacobian matrix allow us to represent the system by two decoupled subsystems: a linear subsystem, which represents the translational dynamic and a non-linear subsystem, which represents the orientation aspects. Therefore, the task of controlling the position and the orientation of the platform may be performed separately. Both subsystem have different properties, in this way we may improve the performance by an individual parametrization of each controller.

6. CONCLUSION

This paper presented a quaternion based model for Stewart platforms, which is a compact model representation of the system. In addition, using its Jacobian matrix, it is possible to transform the linear forces of the six actuators in to forces and torques applied on the center of mass of the top platform, which allow us to describe the system dynamics with decoupled inputs. Following the proposed procedure, representing this system in a Quasi-LPV model allowed us the use of convex mathematical tools, which permitted a systematic way to design the feedback terms K and H by using the LMI framework. Moreover, the proposed control scheme ensured the exponential performance, the system closed-loop stability and the rejection of harmonic disturbances with time-varying fundamental frequency for an admissible set of initial conditions. We also presented in this paper the stability proof of the closed-loop system taking into account the nonlinearities of the platform rotational aspect. In future work, an important and useful contribution would be the addition of the actuator saturation in the control design and its stability proof.

REFERENCES

Castro, R., Salton, A., Flores, J., Kinnaert, M., and Coutinho, D. (2017). Variable frequency resonant controller for load reduction in wind turbines. *Control Engineering Practice*, 66, 76–88. doi:doi.org/10.1016/j.conengprac.2017.06.007.

de Faria, P.F.S.R., Castro, R.S., Salton, A.T., and Flores, J.V. (2016). Quaternion-based dynamic control of a 6-DOF stewart platform for periodic disturbance rejection. In *2016 IEEE Conference on Control Applications (CCA)*. IEEE. doi:10.1109/cca.2016.7587968.

Do, W.Q.D. and Yang, D.C.H. (1988). Inverse dynamic analysis and simulation of a platform type of robot. *Journal of Robotic Systems*, 5(3), 209–227. doi:10.1002/rob.4620050304.

Guo, X., Ke, G., Zheng, F., and Zhang, L. (2013). Forward kinematics analysis of the stewart parallel platform based on the elman recurrent network. In *2013 5th International Conference on Intelligent Human-Machine Systems and Cybernetics*. IEEE. doi:10.1109/ihmsc.2013.189.

Hajimirzaalian, H., Moosavi, H., and Massah, M. (2010). Dynamics analysis and simulation of parallel robot stewart platform. In *2010 The 2nd International Conference on Computer and Automation Engineering (ICCAE)*. IEEE. doi:10.1109/iccae.2010.5451249.

Kim, N.I. and Lee, C.W. (1998). High speed tracking control of stewart platform manipulator via enhanced sliding mode control. In *Proceedings. 1998 IEEE International Conference on Robotics and Automation (Cat. No.98CH36146)*. IEEE. doi:10.1109/robot.1998.680756.

Kumar, P. and Bandyopadhyay, B. (2012). Stabilization of stewart platform using higher order sliding mode control. In *2012 7th International Conference on Electrical and Computer Engineering*. IEEE. doi:10.1109/icece.2012.6471707.

Lee, S.H., Song, J.B., Choi, W.C., and Hong, D. (2003). Position control of a stewart platform using inverse dynamics control with approximate dynamics. *Mechatronics*, 13(6), 605–619. doi:10.1016/s0957-4158(02)00033-8.

Liu, M.J., Li, C.X., and Li, C.N. (2000). Dynamics analysis of the gough-stewart platform manipulator. *IEEE Transactions on Robotics and Automation*, 16(1), 94–98. doi:10.1109/70.833196.

Nguyen, C.C., Antrazi, S.S., Zhou, Z.L., and Campbell, C.E. (1993). Adaptive control of a stewart platform-based manipulator. *Journal of Robotic Systems*, 10(5), 657–687. doi:10.1002/rob.4620100507.

Rotondo, D., Nejjari, F., and Puig, V. (2013). Quasi-LPV modeling, identification and control of a twin rotor MIMO system. *Control Engineering Practice*, 21(6), 829–846. doi:10.1016/j.conengprac.2013.02.004.

Stewart, D. (1966). A platform with six degrees of freedom. *Aircraft Engineering and Aerospace Technology*, 38(4), 30–35. doi:10.1108/eb034141.

Su, Y., Duan, B., Zheng, C., Zhang, Y., Chen, G., and Mi, J. (2004). Disturbance-rejection high-precision motion control of a stewart platform. *IEEE Transactions on Control Systems Technology*, 12(3), 364–374. doi:10.1109/tcst.2004.824315.

Villacis, C., Navarrete, M., Rodriguez, I., Romero, F., Escobar, L., Fuertes, W., Chamorro, S., Benavides, R., Zambrano, M., and Burns, C. (2017). Real-time flight simulator construction with a network for training pilots using mechatronics and cyber-physical system approaches. In *2017 IEEE International Conference on Power, Control, Signals and Instrumentation Engineering (ICPCSI)*. IEEE. doi:10.1109/icpcsi.2017.8392169.